Mechanism of Pore Formation in Reverse Osmosis Membranes During the Casting Process

P. NEOGI

Department of Chemical Engineering
University of Missouri
Rolla, MO 65401

The process of pore formation during the casting of reverse osmosis membranes is analyzed. The process consists of two steps. The first step is the evaporation step, where the cast polymer solution is allowed to dry for 1 ~ 100 s. The second step is the gel formation step, where the cast is soaked in water leaving behind the membrane in form of a gel. The evaporation step gives rise to a thin (~0.1 μm) skin of high density and very small pores which is chiefly responsible for desalination. The gel forms the backing (~100 to 250 μm) and contains large pores.

It is shown that low evaporation rates accompanied by shrinkage during evaporation gives rise to an instability leading to the formation of the skin region. The evaporation effect is fast, is confined to the skin region, and gives rise to very small pores. The gel formation is shown to be a very slow process which cannot interfere with the skin formation due to the vast differences in their rates of formation. It also gives rise to larger pores. All key features of the above experimental observations are explained.

The kinetics of the process depend on the diffusion coefficients D and D_p of the solvent and the polymer. However, the main factor is the solution chemistry of the polymer-solvent system which controls both the effectiveness of the skin and the gel formed. For the first time, the relevant thermodynamic parameters which determine the extent and sizes of pore formation have been obtained.

SCOPE

Separation with membranes is not new, but it still holds promise for wider use in the future. Only asymmetric polymeric membranes are discussed here. Reverse osmosis membranes are made of ionizable polymers like cellulose acetate. In presence of water, the walls of the membrane pores electrify, setting up an electrical field inside the pores. Under these conditions, it is possible to hinder the transport of ions through these pores, and at the same time allow the passage of water. Desalination is thus effected, the success of which depends on the ability of the polymer to electrify as well as on the sizes of the pores. The latter also plays a crucial role in ultrafiltration since the pores do not permit the passage of particles larger than their diameters. Filtration or separation of macromolecules, biological cells, and colloidal particles are thus possible. Consequently, membranes find important application in separation of proteins and enzymes, particularly as these materials are heat-sensitive and the process requires neither heating nor cooling. They also find application in biomedical engineering like in fabrication of artificial kidneys. It is noteworthy that these membranes often have very high separation or rejection efficiencies.

It is evident that the separation takes place due to the existence of pores of desirable radii. Although extensive research has been done on the membrane (and pore) forming properties of a number of polymers, no reliable design criteria have emerged, not even the proper identification of transport or thermodynamic properties of the system that govern the formation of pores. Where mathematical models exist, they contradict experimental observations.

The more difficult task of predicting the pore-size distribution from theory has not been attempted here. Instead, the major parameters that determine whether the pores will form at all or not on fabrication, have been identified from theory. Estimates of times required in the various steps of membrane fabrication have been determined. The theory explains the key features of the experimental observations as well as helps to reduce the numbers and types of fabrication experiments needed to evaluate membrane performance.

CONCLUSION AND SIGNIFICANCE

There are a few controversies shrouding the choice of the solvent and bath liquid for the membrane casting process (Cabasso, 1981). It is seen in the analysis that an optimum solvent exists, where the swelling is not too high nor too low. Thus, although one may in principle strike the right solvent without any difficulties, usually one would need to go through the more torturous route of mixed solvents as in Loeb-Sourirajan membranes. However, the quantitative swelling criteria for solvents have been developed here, which can be used to reject potential solvents. The criteria are too weak to say if solvents acceptable by these are actually acceptable in practice.

It is well known that in some cases ultrashort exposure times are sufficient for the membrane to develop the right type and number of pores (assuming that the solution criteria are satisfied). It is also known that it may take as long as a few minutes. It is seen here that the pores of ~1 nm responsible for salt rejection in reverse osmosis develop instantaneously. Further, it can even develop if the membrane is cast in the bath solution provided that the diffusion coefficient of the solvent in the bath is much greater than that in the polymer. For pores of ~0.1 μm, a few minutes are required. The latter is the upper range of the pore diameters that take part in desalination and do occur in the membrane skin where the actual salt rejection takes place.

The membrane backing is seen to take several hours to form.

0001-1541-83-6878-0402-$2.00.

The differences in the rates of skin and the backing formations are mainly due to the differences in the mechanisms and partly due to the differences in the diffusion coefficients of the polymer and the solvent ($D_p \ll D$).

All key observations on the membrane formation are explained by the model presented here. The prediction of the model that there are wavelike structures on the surface is borne out by electron microscopy measurements. The parameters responsible for pore formation have been identified and in quantitative form.

INTRODUCTION

Separation with membranes provides many attractive features. However, the fabrication of membranes remain as much an art as it was in the days when Loeb and Sourirajan (1963) made the first membrane which could withstand the rigors of a commercial process and answer to its needs. In subsequent sections, attention is focused on the casting of reverse osmosis membranes since this variety is the most sophisticated, encompassing a wide variety of casting processes and end products. All the existing separation processes involving membranes are successful only if they contain pores in a desirable range of pore radii. Consequently, there has been some discussion on how these pores form, since the knowledge of the mechanism would identify the important physico-chemical parameters of the system. Such an analysis is of importance not only for the above reason, but also for the reason that it is a precursor to the more important problem of estimating the pore-size distribution. The existing suggested mechanisms are unsatisfactory for the reasons cited below. Before examining those, it is necessary to examine critically the casting process since that is the stage where the pores are formed.

The Loeb-Sourirajan membrane was made by spreading uniformly a thin layer (~100 to 250 μm) of a solution of cellulose acetate (22.2% by weight), acetone (66.7%), water (10%), and magnesium perchlorate (1.1%) on a glass plate at −10 to 0°C. About 200-s exposure time to air was allowed, after which the plate with the membrane was dipped into ice-water for about 4,000 s. Subsequently, the membrane was peeled off and dipped into hot water for deswelling. Since a very large amount of research has been done in this area, detailed references will not be provided. Some standard texts and reviews are: Sourirajan (1970, 1977), Loeb (1966), Merten (1966), Kesting (1971), Turback (1981), Cooper (1980), Lonsdale and Podall (1972). These cover the entire background material. Where exceptions exist, references have been cited.

One of the striking features of the membranes formed by the above process is their asymmetry. This could be deduced from the performance and the surface texture (Sourirajan, 1970) but was verified without doubts with the electron microscope (Riley et al., 1964, 1966). The surface, which is exposed to air on casting, develops ~0.1-μm-thick, high-density layer. It contains very small pores of radii ~1 nm (Sourirajan, 1970; Lonsdale, 1966). The rest of the membrane contains relatively larger pores. It was also shown that it was this high-density layer that gives the membrane its ability to reject salts. The large backing provides it with mechanical strength. The latter is necessary since the membrane has to withstand pressure drops in the range of 7 MPa for desalination. For proper ion retention, it is necessary for the membrane to have pores with diameters in the range of 0.3 to 5 nm. This is supplied in the high-density skin. Because of the smallness of the diameters of the pores, the skin also provides a major resistance to the flow of water through it. To improve the flow of water through the membrane, the backing should have relatively larger, well-defined and interconnected pores. Because ionizable groups on the pore walls are required for ion retention, cellulose acetate forms a very suitable material. Subsequent discussions are confined to cellulose acetate membranes, even though the analysis covers wider varieties.

Much of the membrane structuring is accomplished through a proper selection of the solvent. Usually a mixture is used to get the required solvent properties, like acetone-water, acetone-formamide, etc., together with solvating inorganic salts, like magnesium perchlorate, zinc chloride, etc. Since the relative concentration ratio of polymer: solvent and the temperature, have important effects on solvation, these form important variables in the casting process. The solution at lower polymer contents form sols and higher polymer contents form gels. Gels are characterized by degrees of molecular order. The membrane that is left behind is in the form of gel. It is observed that gels that are precipitated from solutions of poor solvents give rise to good structure in the backing material. However, its ion retention is low (Kesting, 1971). One needs to have an intermediate solvent. For cellulose acetate membranes, acetone-water mixture is used. This is a poor solvent. Its ability to solvate the polymer is increased by adding magnesium perchlorate or other swelling agents. This provides the correct mix of solvating property and volatility (Sourirajan, 1970). That evaporation has an important role in the formation of the skin has been demonstrated (Sourirajan, 1970; Loeb and Sourirajan, 1963). Larger evaporation times give rise to membranes with poorer performance.

Before discussing the proposed model or the existing ones, it is necessary to examine the casting processes in more detail.

FURTHER DISCUSSIONS ON MEMBRANE CASTING

Membrane casting is characterized by two important steps (and then a third which is necessary for making it suitable for desalination). The first two steps are the evaporation and the stage where it is soaked in ice-water. The two steps have two representative time scales: evaporation 10 s to 100 s and soaking ~4,000 s. For the purpose of bringing out the diverse natures of casting processes, a few representative types are listed.

(a) *Loeb-Sourirajan membrane.* The membrane is cast from a solution containing ~22 wt. % polymer. The casting is done at freezing or below freezing temperatures. The times of evaporation run up to 200 s, after which the membrane is soaked in ice-water for an hour.

(b) *Sirkar et al. (1978).* The membrane is cast from a solution containing ~30 wt. % polymer. The casting is done at room temperatures. The times of evaporation are as low as 0.01 to 10 s, after which the membrane is soaked in ice-water for an hour. Better salt retentions are reported.

(c) *Ultrathin membranes (Sourirajan, 1970).* A glass plate is withdrawn very slowly from a pool of very dilute solution of cellulose acetate. A layer of polymer is deposited on the plate and eventually dries into the membrane. Immersion into ice-water bath is not necessary. The membranes are ultrathin (~1 μm), high density, and with high salt rejections. Thus, it is as though only the skin of the membrane is cast.

Some important features can be summarized as:

(i) The skin formation is enhanced if the evaporation rate of the solvent is decreased by some extent. In Loeb-Sourirajan membranes, this is done by decreasing the casting temperatures. In Sirkar et al. (1978) type membranes, this is done by increasing the polymer content. A practical limitation exists in either method; *viz.*, the viscosity of the solution can become too high for the membrane to be cast.

(ii) Evaporation affects only a thin layer at the surface. This is proven through membrane (c), where the necessary condition for the formation of high-density membranes is that they be ultrathin.

For thick membranes, increased evaporation times only deteriorate the membranes.

Anderson and Ullman (1973) identified the diffusion of the solvent in the polymer as the primary reason for the formation of the skin region. The fact that such diffusion processes are strongly dependent on the solvent concentration and relaxation times is well known (Ueberreiter, 1968, Vrentas and Duda, 1979) and could very well enhance the asymmetry in the membranes as shown by them. However, the origin of pores is not treated in their model. Such an attempt has been made by Kesting (1971). Since the solvent evaporates, the solution precipitates gels. Patches of gels and almost clear solvent are formed. The latter is leached out on immersion into the ice-water bath leaving behind clear pores. Since, at the surface, the rate of solvent depletion is large, the solution smoothly turns to gel, at a rate faster than the rate of precipitation of the gel. Further, as the gel has a higher density, it contracts and cracks open on the surface leaving small pores.

It is interesting to note that Kesting's mechanism looks at the migration of polymer molecules; that is, the growth of gel patches under a driving force which is the gradient of chemical potential. Both Anderson and Ullman (1973) and Kesting (1971) identified the shrinkage of the cast material under evaporation as another mechanism for the bodily movement of the polymer, its potentials were not explored.

Stevens and others (Stevens et al., 1980; Petty and Stevens, 1980; Stevens, 1976) and Cohen, Tanny and Prager (1979) have attempted to model the problem, concentrating for the first time on the pore formation itself. Petty and coworkers assume that the skin is formed due to the surface tension driven instabilities. Such instabilities on the evaporating interfaces leave clear hexagonal patterns (Miller, 1978). Such patterns are not seen on the membrane surface under the electron microscope; instead, randomly arranged waves of sizes larger than the pore diameters are observed (Katoh and Suzuki, 1981). They also argue that the backing is formed in the bath where the bath water (poor solvent) replaces acetone in the membrane causing supersaturation. On supersaturation the gel immediately precipitates. The difficulty arises on noting that the precipitation requires actual migration of polymer molecules through diffusion. In its entangled form in high-concentration sols, the diffusivity of the polymer will be very small. Thus, not only the rate of precipitation will be lower than the rate of formation of supersaturation, it will probably be the controlling factor. This was recognized by Cohen et al. (1979) who included both the rate of formation of the supersaturation and the kinetics of phase change in their model. The phase change from sol to gel was assumed to take place not through nucleation and subsequent growth of the nuclei (precipitation) but through spinodal decomposition, i.e., spontaneous decomposition from a thermodynamically unstable composition.

The model suffers for the following reasons. First, due to the fact that it stresses the phase behavior (acetone-water-cellulose acetate ternary diagram) and only through it the swelling properties of the system, although the latter is known to critically govern the pore formation (Cabasso, 1981). Secondly, in the sol, the nuclei are already present and will promote phase change through the growth of the nuclei rather than through spinodal decomposition. This will be discussed later in detail. Thirdly, it provides no direct means of explaining the waves (bumps) on the surface seen by Katoh and Suzuki (1981).

Even though quantitative experimental results are few against which a theory may be checked, sufficient experimental observations exist to evaluate the models. The above models either lack quantitative analyses or contradict experimental observations. In the following sections a mechanism is proposed and analyzed. It attempts to explain the motivations behind the diverse methods of membrane casting and their effects. Since an analysis is provided it is possible to evaluate the model. A difficulty is encountered that relevant physical data could not be obtained. However, with reasonable estimates it is shown that the model can explain all key features quantitatively. For the first time, thermodynamic and transport properties are identified, which if known can predict the nature of the membrane.

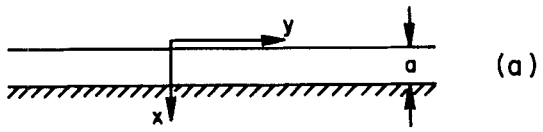

Figure 1a. Coordinate systems used in the stability analysis of skin formation.

MODEL

It is assumed that the gel is formed by precipitation from a supersaturated polymer solution. However, the formation of the gel is very slow compared to the rate of formation of the skin.

While drying, the system receives random disturbances. It is shown that such disturbances can grow in the skin during the evaporation stage, if the rate of evaporation is slow and is accompanied by a decrease in volume. Any disturbance can be broken down into waves of different amplitudes and frequencies. The important feature is that these growing disturbances deepen into pores. If the disturbances with smallest wavelengths grow most rapidly, then most pores would be small. One supposes that the growth of pores should decay rapidly with time and decay with the penetration into the film. These would explain the observations if it could be shown that the rate of growth of the gel is extremely small compared to the rate of growth of pores in the skin. As mentioned previously, this would ensure that the solution smoothly solidifies into the skin.

It is assumed that in the backing gel forms through growth of gel nuclei in a supersaturated solution. This supersaturated phase is formed due to low temperatures in the ice-water and moderately fast replacement of the original solvent by water, which is a poor solvent. The growth of the gel nuclei is controlled by the diffusion coefficient D_p of the polymer in the solution. Since the D_p is extremely small, the times taken for the formation of the membrane gel are very large and expected to be in the range of hours.

SKIN FORMATION

A layer of polymer solution of thickness a is cast on a surface, Figure 1a. The solution is assumed to be of two components; here it will be assumed to be of cellulose acetate-acetone. The acetone evaporates into air. The diffusion coefficient of acetone in air is very high 10^{-5} m^2/s, compared to the diffusion coefficient of acetone in the solution. The latter can be estimated to range from 10^{-10} to 10^{-16} m^2/s (Ueberreiter, 1968). Consequently, the concentration of acetone at the surface is extremely low. The basic evaporation rates can be obtained.

Base Case

The coordinates are shown in Figure 1a. The concentration varies only in the normal x-direction, and the origin is located on the surface. The rate of shrinkage due to evaporation is neglected as the first approximation. Since the diffusion coefficient of acetone in the polymer is very small, in the short evaporation times under consideration, it is assumed that the concentration in the polymer is at the initial value c_o except for a small layer at the boundary. The conservation equation and the initial and boundary conditions are

$$\frac{\partial c}{\partial t} = \frac{\partial}{\partial x}\left[D\frac{\partial c}{\partial x}\right] \tag{1}$$

$c = c_o$ (initial concentration) (2)
at $t = 0$

$c = c_o$ (boundary layer is small) (3)
at $x \to \infty$

$c = 0$ (diffusion in the solution (4)
at $x = 0$ limited transport)

In the last condition, Eq. 4, it has been assumed that since the diffusion coefficient of the acetone in air is very high, the acetone concentration at the polymer-air interface is practically zero.

Assuming diffusion coefficient of the solvent D, to be a constant, solution to Eq. 1 subject to Eqs. 2–4 becomes

$$c = c_o \text{ erf}\left[\frac{x}{\sqrt{4Dt}}\right] \tag{5}$$

where *erf* is the error function. The rate of change of the membrane thickness can be obtained from the conservation of the nonvolatile polymer,

$$\frac{d}{dt}\int_0^{a(t)} \rho_p dx = 0 \tag{6}$$

here ρ_p is the molar density of the polymer in the solution and is equal to $(\rho - c)$, where ρ is the total molar density. Using Leibnitz's rule of differentiation and the chain rule, Eq. 6 becomes

$$\int_o^a (\rho_c - 1)\frac{\partial c}{\partial t}dx + (\rho - c)\Big|_{\substack{x=a \\ (c=c_o)}} \dot{a} = 0 \tag{6a}$$

where $\rho_c = \partial\rho/\partial c$. Assuming ρ_c to be a constant, and substituting Eq. 1 for $\partial c/\partial t$,

$$-D(\rho_c - 1)\frac{\partial c}{\partial x}\Big| + (\rho - c)\Big|_{\substack{x=0 \\ (c=c_o)}} \dot{a} = 0 \tag{6b}$$

is obtained. In Eq. 6b, the term $\partial c/\partial x$ at $x = a$ has been neglected in keeping with the earlier assumption that the concentration gradients are confined to the surface region. Using Eq. 5, Eq. 6b becomes

$$\dot{a} = \left[\frac{\partial \ln(\rho - c)}{\partial \ln c}\right]\Bigg|_{c=c_o} \frac{\sqrt{D}}{\pi t} \tag{7}$$

In Eq. 7, since $(\rho - c)$ increases with decreasing c, the term $[\partial \ln(\rho - c)/\partial \ln c]$ is negative; thus, $\dot{a}$ is negative, implying a shrinkage. In the above analysis, the flow and convective effects have been taken to be very small, since the viscosity is very high. The polymer moves only through shrinkage.

Stability Analysis

The mechanisms through which the evaporating vapor-liquid interface become unstable is shown in Figure 1b. A disturbance on the interface in form of a wave is shown. The disturbance takes place due to uneven shrinkage. Since the diffusion coefficient D is very small, the concentration increases sharply from its value of zero at the interface. Thus, when the disturbance takes place, the concentration gradient on the crest P is much lower than the concentration gradient in the trough P'; consequently, the rate of evaporation at the trough is high. As in this case, when evaporation is accompanied by a decrease in volume, the trough deepens with respect to the crest.

In the above process, although the distance through which the acetone must diffuse through the polymer in the trough region is decreased, the accompanying distance through the air is increased. For the trough to deepen with respect to the crest, it is necessary that the diffusional resistance in the polymer be substantially higher than that in the air. This condition is always met, and it is noteworthy that the pore-forming ability is enhanced on increasing the diffusional resistance in the polymer which decreases the base evaporation rate. This last point has been noted earlier. It is also unnecessary to cast the membrane in air, as long as the diffusivity D of the solvent in the polymer is much less than the diffusivity of the solvent in the surrounding medium. Thus, it has been noted by Cabasso (1981) that acceptable membranes can also be formed by quenching them directly in the bath.

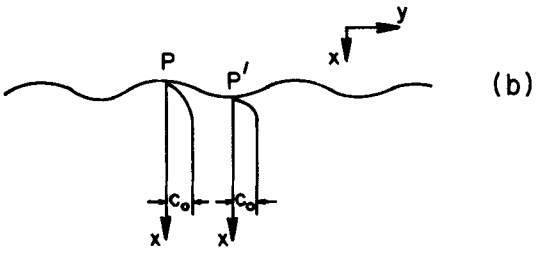

Figure 1b. Effects of a disturbance in form of a wave on the surface. The concentration gradient in a trough (P') becomes steeper.

In the linear stability analysis that will be undertaken here, it will be assumed that the system receives arbitrary but small disturbances from outside. The latter assumption makes linearization possible. The sources of disturbances are many, one may for instance cite the action of the rollers. Now, it is important to recognize that fluctuations in the membrane thickness due to the disturbance gives rise to fluctuations in the concentration since the two are related through the principle of conservation of mass. Thus, under these disturbances, all quantities are perturbed from the base values obtained in the previous section, and all such perturbations are related in a unique way whatever be the source of the disturbance.

In the analysis below, the perturbed quantities have been denoted with primes. Thus, the concentration c in the previous section becomes $c + c'$, where c' is the perturbed quantity. The new variables $c + c'$ and $a + a'$ are substituted in Eqs. 1–4 and 6. Since c and a themselves satisfy Eqs. 1–4 and 6, these are used to simplify the new equations, giving rise to the conservation equation

$$\frac{\partial c'}{\partial t} = D\left[\frac{\partial^2 c'}{\partial x^2} + \frac{\partial^2 c'}{\partial y^2}\right] \tag{8}$$

The vapor-liquid interface is at $x = a'$. The boundary conditions there are expanded in a Taylor's series about $x = 0$, and only linear terms are retained. One has

$$c' + \frac{\partial c}{\partial x}a' = 0 \qquad \text{on } x = 0 \tag{9}$$

$$c'\Big|_{x\to\infty} = 0 \tag{10}$$

The perturbations may be taken in all generality. However, any perturbation can be expressed in terms of Fourier series. The disturbances are broken down into waves of different and unknown amplitudes. Only the disturbance corresponding to an arbitrary wave number ω (or wavelength $\Lambda = 2\pi/\omega$) is analyzed; that is, with $c' = \hat{c}(x)e^{i\omega y}e^{\beta t}$ and $a' = \hat{a}e^{i\omega y}e^{\beta t}$, where for simplicity the disturbances have been assumed to exist only in x- and y-directions. As a part of the solution, β is obtainable as a function of ω. Thus, if for a disturbance of wavenumber ω, $\beta < 0$, such disturbances will disappear with time. The system is then stable with respect to disturbances of that particular wavenumber. If, however, $\beta > 0$, the form of c' and a' assures us that the amplitudes increase with time. The system is then said to be unstable to disturbances of such wavenumbers leading to the formation of pores. Substituting for c' and a' in Eqs. 8–10, the solution is obtained as

$$\hat{c} = \frac{-c_o\hat{a}}{\sqrt{\pi D t}}\exp\left(-x\sqrt{\omega^2 + \frac{\beta}{D}}\right) \tag{11}$$

The conservation equation for the polymer, Eq. 6a, modifies to

$$\frac{d}{dt}\int_{-\infty}^{\infty} dy \int_{a'}^{a} (\rho + \rho' - c - c')dx = 0 \tag{12}$$

using same procedure as before, and Eqs. 6a and 8, one obtains,

$$\int_{-\infty}^{\infty} dy\left[(\rho_c - 1)D\int_o^a \left(\frac{\partial^2 c'}{\partial x^2} + \frac{\partial^2 c'}{\partial y^2}\right)dx - (\rho - c)\Big|\dot{a}'\right] = 0 \qquad x = 0$$

where the fact $\partial^2 c/\partial x^2| = 0$ has been used. Substituting for c' and a', $0 = x$

$$(\rho_c - 1)\frac{c_o}{\sqrt{\pi Dt}} \cdot \frac{\beta}{\sqrt{\frac{\beta + \omega^2}{D}}} + (\rho - c)|\beta = 0 \qquad (13)$$
$$x = 0$$

is obtained. Rearranging, one has

$$\beta = \left(\frac{\kappa^2}{\pi Dt} - \omega^2\right) D \qquad (14)$$

Firstly it is seen that β can be greater than zero only because of the term κ which is

$$\kappa = -\left[\frac{\partial\, ln\, (\rho - c)}{\partial\, ln\, c}\right] \cdot \frac{\rho_p(c = c_o)}{\rho_p(c = o)} \qquad (15)$$

Secondly, Eq. 13 has also to be satisfied. Rearranging Eq. 13 one has

$$\frac{\sqrt{\beta + \omega^2}}{D} = \frac{\kappa}{\sqrt{\pi Dt}} \qquad (15a)$$

Note that κ has to be positive for β to be positive and real. As mentioned previously, the term $\partial\, ln\, (\rho - c)/\partial\, ln\, c$ in Eq. 15 is expected to be negative and thus κ is indeed positive. In deriving Eq. 13, the values $\hat{c}(x = a)$ and $d\hat{c}/dx_{x=a}|$ have been neglected as appropriate for the thin concentration boundary layer assumed here.

Results

It is immediately seen in Eq. 14 that the condition under which disturbance of a particular wavenumber will grow ($\beta > 0$) is given by $\kappa^2/\pi Dt > \omega^2$, that is, all wavenumbers smaller than $\sqrt{\kappa^2/\pi Dt}$. It is also seen that the growth of an initially developing wave ceases with time ($\beta \to 0$). Since a growing disturbance of wavelength Λ (wavenumber $\omega = 2\pi/\Lambda$) deepens into pores of diameters $\Lambda/2$, ultrafine pores of diameters ~1 nm can be formed only at short times. Further, the growth time τ_g, through which a disturbance of a given wavelength grows ($\beta \geq 0$) is obtained by setting $\beta = 0$ in Eq. 14. The result is

$$\tau_g = \left(\frac{\Lambda}{2}\right)^2 \frac{\kappa^2}{\pi^3 D} \qquad (16a)$$

that is, the disturbance grows from time $t = 0$ to $t = \tau_g$.

The question now arises that if in the time available, the disturbance of a given wavelength would grow sufficiently to deepen into a pore. This is answered through the examination of the amplitude of the disturbance, $a' = \hat{a}e^{i\omega y}e^{\beta t}$. The amplitude is proportional to $e^{\beta t}$ and is considered in linear stability analysis to be fully grown if $\beta t \sim 0(1)$, that is the time dependent contribution $e^{\beta t}$ is then sufficiently large. Obviously this is no more than an estimate. One defines a time τ when the disturbances are fully grown, as $\beta\tau = 1$, or from Eq. 14,

$$\tau = \left(\frac{\Lambda}{2}\right)^2 \frac{(\kappa^2/\pi - 1)}{D\pi^2} \qquad (16b)$$

Comparing Eqs. 16a and 16b, it is seen that the time for development $\tau < \tau_g$ the total time of growth. Finally for the physically realistic case, $\tau > 0$, or from Eq. 16b

$$\kappa > \sqrt{\pi} \qquad (17)$$

Equation 17 provides a constraint on the solution thermodynamics.

It is necessary to point out the shortcomings of Eq. 17. Since it has been obtained from linear stability analysis which is valid initially, the analysis has been confined to the evolution of the disturbances that occur initially, that is, at time $t = 0$. The disturbances that occur at later times are allowed smaller times for growth. Thus the condition in Eq. 17 assures one that only the disturbances that arrive at time $t = 0$ grow into pores. However, it does not say whether those that arrive at later times grow into pores or not. Since the pores that develop from disturbances that arrive later than at $t = 0$ may be necessary to give the membrane adequately large number of pores, and since these can form only if κ is large, these mean that in reality κ is larger than that suggested by Eq. 17.

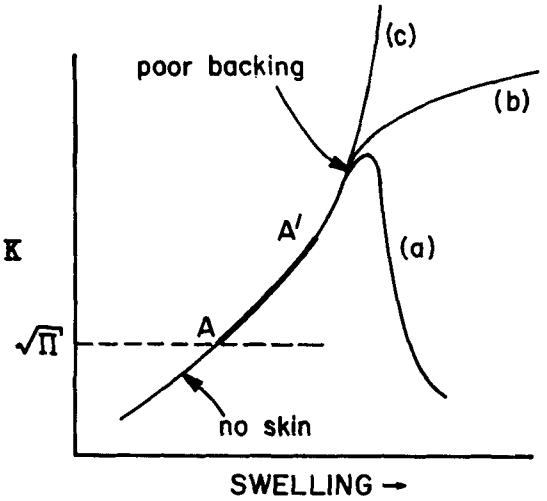

Figure 2. Range AA' where a proper reverse osmosis membrane can be cast. $\kappa > \sqrt{\pi}$ is needed for the skin formation. Too high swelling is bad for the backing. The cases (a), (b) and (c) represent possible behavior of κ.

Examining κ further (Eq. 15), one notes as before that the term $-[\partial\, ln\, (p - c)/\partial\, ln\, c]$ is positive and increases with the increasing ability to swell the polymer. However, the term $\rho_p(c = c_o)/\rho_p(c = 0)$ decreases. Consequently, as shown in Figure 2, κ may pass through a maximum with increasing swelling ability of solvents. For the skin to occur, κ is required to be $> \sqrt{\pi}$. It has been mentioned previously that for good backing formation the swelling ability should not be large. Thus, only the portions marked A A' in Figure 2 gives rise to a proper membrane. Proper data on κ could not be obtained, except for one set of values on densities of cellulose acetate-acetone solution at 30°C (Moore, 1971). From the data, κ was calculated and found to lie between 0.1 to 1. This is below the value of $\sqrt{\pi}$ but not too far away. This result is not surprising since acetone alone gives rise to an unacceptably poor membrane (Sourirajan, 1970).

Since a growing disturbance of wavelength Λ can deepen into a pore of diameter of about $\Lambda/2$, Figure 3a, τ has been plotted

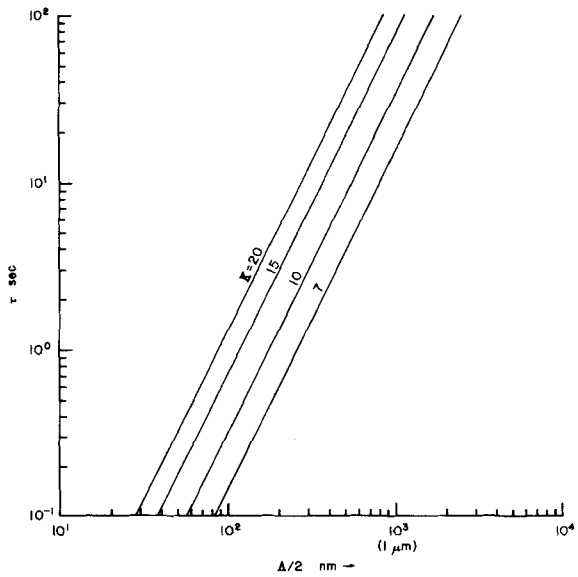

Figure 3a. Pore formation times τ in the skin has been plotted against $\Lambda/2$ which is the length representing a pore diameter. A value of $D = 10^{-13}$ m²/s and various values of κ as shown have been used (Eq. 16b).

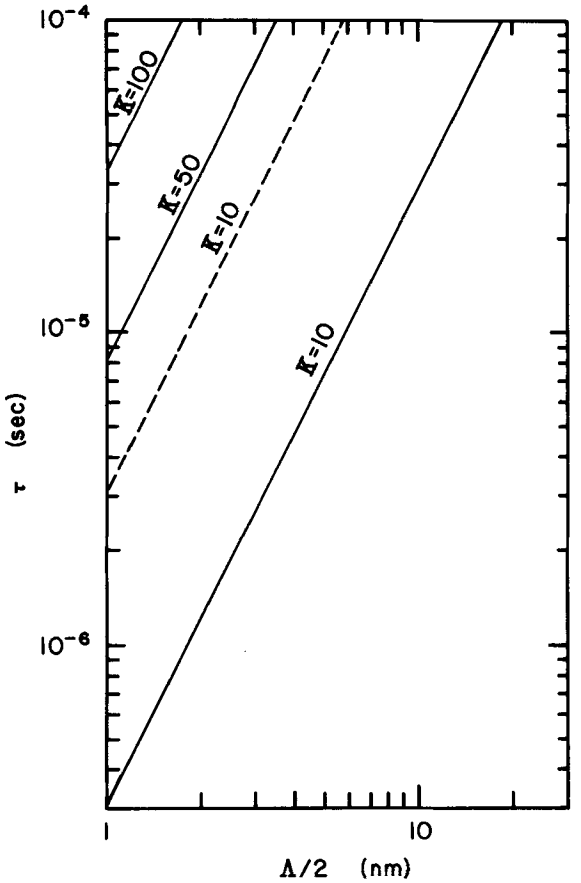

Figure 3b. Formation times τ for pores with diameter ~1 nm, that is, $\Lambda/2 \sim$ 1 nm. The bold lines are for $D = 10^{-11}$ m²/s and the dashed line is for $D = 10^{-12}$ m²/s.

against $\Lambda/2$ for various values of κ and $D = 10^{-13}$ m²/s. Equation 16b has been used to draw the plots. Increasing the values of κ or decreasing D, increases the times to reach pores of a particular length scale. This is apparent from Eq. 16b. If the evaporation times run from less than a second to a minute, then pore sizes range up to ~1 μm. The times of pore formation of diameters ~1 nm are shown in Figure 3b. The speed is seen to be extremely high. The results on pore size ~1 nm may not be reliable since continuum formalism cannot be used. However, the results do indicate virtually instantaneous response on the molecular scale.

It is also important to have some estimate for ℓ the thickness of the skin since correlations exist relating ℓ to the membrane performance (Sirkar, 1977). In Eq. 11, it is observed that the disturbance disappears in the interior as $\exp(-x\sqrt{\omega^2 + \beta/D})$. Hence these disturbances can be expected to be confined to thicknesses ℓ such that $\ell\sqrt{\omega^2 + \beta/D}$ is large and the exponential term is small. Setting this term to 1 we have, using Eqs. 15a and 16b,

$$\ell = \frac{\Lambda}{2\pi}\left(1 - \frac{\pi}{\kappa^2}\right)^{1/2} \tag{18}$$

where $\kappa^2 > \pi$ from Eq. 17. Thus, $\ell < \Lambda/2\pi$, and if the largest pore sizes $\Lambda/2 \sim 1$ μm, the skin thicknesses are <1 μm. In the usual cases where $\ell \sim 0.1$ μm (Lonsdale, 1966), it implies that 0.1 μm is approximately the largest pore size available.

Finally, in the Appendix, the analysis is extended to include two-component solvents and a nonvolatile solvating agent. No additional information is obtained, except that it is seen that a greater degree of freedom is available in constructing a proper mixed solvent.

Thus, the key features of the skin formation are explained. It has been shown that the solvent should evaporate slowly and should swell the polymer adequately. The evaporation step is shown to take 1–100 s and the size of the pores formed are of the order of less than 1 μm. Further, increasing evaporation times unnecessarily gives rise to pores of large diameters which is known to bring down the ion retention properties of the membrane. As mentioned previously the reverse osmosis membranes reject salts during desalination due to pores ~1 nm in the skin. Figure 3b shows that such pores are formed instantaneously. This is keeping with the results of Sirkar et al. (1978) who allowed very small exposure times—down to 0.01 s—and still obtained good desalination membranes. (The 0.01 s exposure was the minimum that their equipment was capable of.) Further, since the disturbances of smaller wavelengths develop first (Eq. 16b), the smaller ones develop into pores, the larger ones form bumps and the largest would be beyond the scale of measurement. This has been noted by Katoh and Suzuki (1981) in their observations under the electron microscope.

FORMATION OF THE BACKING GEL

It is assumed that the gel is formed mainly in the ice-water bath due to precipitation and growth of the nuclei from a supersaturated solution. This growth of nuclei is the rate limiting step, limited by the diffusion coefficient D_p of the polymer. As noted earlier, the movement of polymer molecules occur through a driving force which is the gradient of chemical potential. The diffusional flux of the polymers is extremely difficult to model (Vrentas and Duda, 1979). Thus, the diffusion coefficient D_p of polymer molecules will be taken to be a constant. Although the assumption appears to be drastic, it preserves the basic nature of the movement of the polymer. In the high concentration solution, D_p is expected to be extremely low (Ueberreiter, 1968), much lower than the diffusion coefficient D of the small solvent molecules. Since the lower reaches of D is of the order of 10^{-16} m²/s, D_p can be assumed to be no smaller than 10^{-16} m²/s. Thus, the times of gel formation can be *a priori* assumed to be extremely high and the rates extremely low.

Since the diffusion coefficient of the solvent(s) is much higher than D_p, the solvent is in equilibrium. The supersaturation occurs both because the ice-water bath temperatures are very low and because the bath liquid (water) replaces the original solvent instantaneously (relatively) and as water is a very poor solvent, the polymer concentration is above saturation.

Due to the fact that the rate of growth of the nuclei is very small, it can be assumed that all nuclei are *formed* initially. It is known that even diluted solutions of cellulose acetate (~1 wt. %) carries microscopic patches of gel (Moore, 1971; Sourirajan, 1970). Further nucleation is facilitated by the presence of inorganic salts. It is assumed that the number of nuclei do not change with time.

The problem now reduces to a moving boundary mass transfer problem. Obviously this is a highly simplified picture, although the basic mechanism of gel formation mechanism is retained. An additional condition exists that as the nuclei grow the polymer content of the solution depletes with time. The exact problem is very difficult to solve, however, the ingeneous approximate solution obtained by Wert and Zener (1950) makes that unnecessary.

Solution

The flux J_p at the surface of a particle is

$$J_p = \frac{\rho_{pg}}{A}\frac{dv}{dt} \tag{19}$$

where A and v are the surface area and the volume of a growing nucleus. If $b(t)$ is its radius, $A = 4\pi b^2$ and $v = 4/3\pi b^3$. Equation 19 becomes

$$J_p = \rho_{pg}\frac{db}{dt} \tag{20}$$

where ρ_{pg} is the molar density of the polymer in the gel (nucleus). J_p is also

$$J_p = D_p \left.\frac{\partial \rho_p}{\partial r}\right|_{r=b} \tag{21}$$

where r is the radius in spherical coordinates with its origin at the center of the spherical nucleus. If n, the number of nuclei per unit volume is adequately low, the boundary layers of two neighboring nuclei do not intersect. Thus under quasistatic conditions the conservation equation in the solution becomes

$$\frac{1}{r^2}\frac{\partial}{\partial r}\left(r^2\frac{\partial \rho_p}{\partial r}\right) = 0 \tag{22}$$

subject to the boundary conditions that

$$\rho_p\Big|_{r=b} = \rho_{pe} \quad \text{(Concentration in the solution in equilibrium with gel, i.e., the solubility of the polymer)} \tag{23}$$

$$\rho_p\Big|_{r\to\infty} = \rho_p^*(t) \quad \text{(Concentration in the bulk away from the nucleus)} \tag{24}$$

The solution is

$$\rho_p = \rho_p^* - (\rho_p^* - \rho_{pe})\frac{b}{r} \tag{25}$$

An average $\langle \rho_p \rangle$ can be found, defined by the balance

$$\rho_{po} - \langle \rho_p \rangle = n\rho_{pg}\left(\frac{4}{3}\pi b^3\right) \tag{26}$$

where $n(4/3\pi b^3) \ll 1$ and ρ_{po} is the initial concentration of the polymer in the solution. If it is assumed that ρ_p far from a nucleus is $\approx\langle \rho_p \rangle$, $\rho_p^* \approx \langle \rho_p \rangle$. Defining conversion X with

$$1 - X = \frac{\langle \rho_p \rangle - \rho_{pe}}{\rho_{po} - \rho_{pe}} \tag{27}$$

one has,

$$\frac{dX}{dt} = -\frac{1}{(\rho_{po} - \rho_{pe})}\frac{d}{dt}\langle \rho_p \rangle \tag{28a}$$

Replacing $\langle \rho_p \rangle$ in Eq. 28a from Eq. 26

$$\frac{dX}{dt} = \frac{n\,4\pi\rho_{pg}}{\rho_{po} - \rho_{pe}} b^2\frac{db}{dt} \tag{28b}$$

is obtained.

Eliminating db/dt in Eq. 28b with Eqs. 20, 21, and 25, and b^2 with Eq. 26, and using Eq. 27, one has

$$\frac{X^{-1/3}}{[1-X]}\frac{dX}{dt} = [48\pi^2(\rho_{po} - \rho_{pe})/\rho_{pg}]^{1/3} n^{2/3} D_p \tag{29}$$

Equation 29 has to be integrated numerically. Instead of doing that, the asympototic solution of Wert and Zener (1950) for large X can be used (see also Fine, 1964). Thus, at advanced stages of gel formation

$$t = -\frac{ln\,(1-X)}{2[48\pi^2(\rho_{po} - \rho_{pe})/\rho_{pg}]^{1/3} n^{2/3} D_p} \tag{30}$$

and

$$\tau = \frac{0.5\,ln\,(2)}{[48\pi^2(\rho_{po} - \rho_{pe})/\rho_{pg}]^{1/3} n^{2/3} D_p} \tag{31}$$

where τ is the time required for 50% of the polymer to turn into gel.

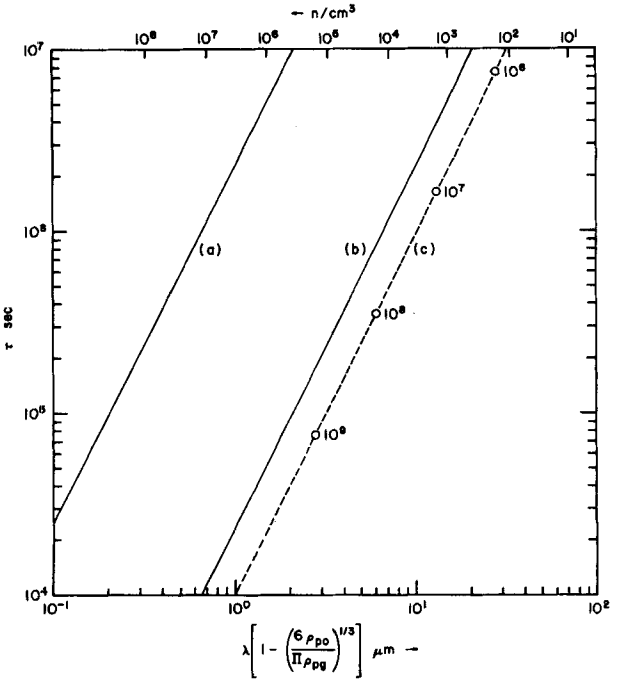

Figure 4. Backing formation times τ for completion of half the gel formation has been plotted against representative pore dimension $\lambda[1 - (6\rho_{po}/\pi\rho_{pg})^{1/3}]$. Values used are: (a) $D_p = 10^{-16}$ m²/s and $\rho_{po}/\rho_{pg} = 0.5$; (b) $D_p = 10^{-14}$ m²/s and $\rho_{po}/\rho_{pg} = 0.5$; and (c) $D_p = 10^{-16}$ m²/s and $\rho_{po}/\rho_{pg} = 0.2$. For cases (a) and (b), the nuclei densities n have been shown at the top. In (c), n has been shown on the plot. ρ_{pe} is zero in all cases. Although $D_p = 10^{-14}$ m²/s is an unrealistic value, it has been shown for comparison.

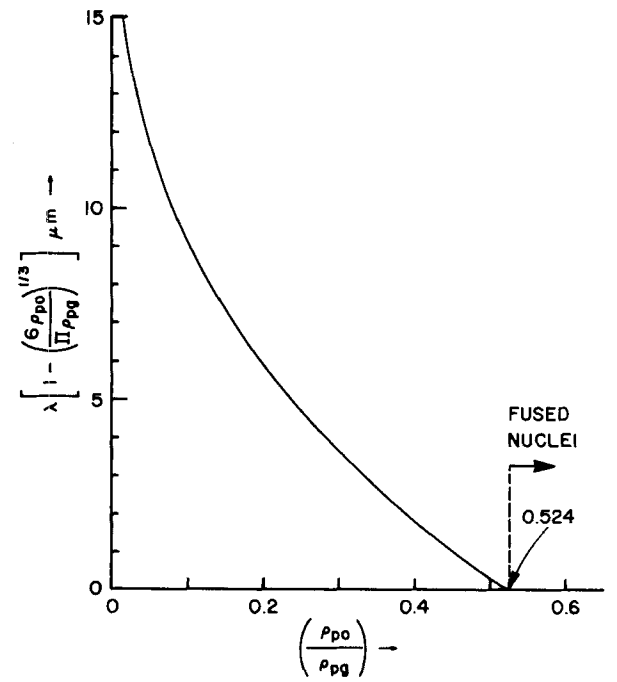

Figure 5. Representative pore length scale in the backing $\lambda[(1 - (6\rho_{po}/\pi\rho_{pg})^{1/3}]$ has been plotted against ρ_{po}/ρ_{pg}. For $\rho_{po}/\rho_{pg} > 0.524$ ($= \pi/6$), the nuclei fuse and more blocked pores are obtained.

Results

A very important conclusion can be drawn from the nature of n, the equilibrium number of nuclei per unit volume. If λ is the average center-to-center distance between nuclei, it would also be a scale representative of the pore sizes. One may write that

$$n \simeq \lambda^{-3} \tag{32}$$

The largest possible number of nuclei per unit volume is n_t, the number of polymer molecules per unit volume. For a 30% cellulose acetate solution of molecular weight $\sim 10^5$ and density $\sim 10^3$ kg/m³, n_t works out to $\sim 10^{18}$ per cm³. Hence, $\lambda >>> 10$ nm; 10 nm belongs to the upper reaches of the pore sizes formed in the evaporation stage. The pore sizes are better estimated as $\lambda - 2b|_{t\to\infty}$. Since $t \to \infty$, $\langle \rho_p \rangle \to 0$, from Eq. 26, $b \to \lambda(3\rho_{po}/4\pi\rho_{pg})^{1/3}$. Thus, the pore sizes $\sim\lambda[1 - (6\rho_{po}/\pi\rho_{pg})^{1/3}]$. Estimates of n are difficult to obtain. For the metallurgical systems studied by Wert and Zener (1950), $n \sim 10^4$ per cm³. For sucrose in water and other

similar solvents n ranges from 10 to 10^8 per cm^3 (van Hook, 1961). In all it may be estimated that n lies from 10^2 to 10^8 per cm^3, that is $\lambda \sim 0.1$ to 10^3 μm. In Figure 4, τ has been plotted against $\lambda[1 - (6\rho_{po}/\pi\rho_{pg})^{1/3}]$ from Eq. 31. It is seen that the times for gel formation are very high, being $\gg 10^5$ s. One supposes that this could be decreased by submerging the membrane subsequently in hot water bath and hence increasing the value of D_p.

As mentioned previously an important criterion in the backing formation is the extent of swelling in the gel (Kesting, 1971). In Figure 5, the pore size estimates

$$\lambda\left[1 - \left(\frac{6\rho_{po}}{\pi\rho_{pg}}\right)^{1/3}\right]$$

have been plotted against (ρ_{po}/ρ_{pg}). Since ρ_{po} and ρ_{pg} are the polymer densities in the casting solution and the final gel respectively, $\rho_{po}/\rho_{pg} < 1$ increasing with increased amount of swelling in the gel. In Figure 5 it is seen that the pore dimension decreases with increased swelling in the gel. If

$$\left(\frac{\rho_{po}}{\rho_{pg}}\right) > \frac{\pi}{6} (=0.524), \tag{33}$$

then the neighboring nuclei will fuse and blocked pores will form. This substantiates the observation that solvents which give swollen gels (good solvents) give rise to poor backing with irregular and walled-up pores.

SUMMARY

It is shown that the evaporation combined with the decrease in volume gives rise to the pores in the skin. The pores are small and they grow for only short times. The orders of magnitude of the pore sizes, the skin thicknesses, and the evaporation times agree well with the experiments. A factor κ related to the polymer swelling is identified which is of great importance. Too low values of κ (low swelling) prevent the formation of the skin. High swelling causes the formation of poor backing material. The times of formation of the gel backing calculated from estimated values of the parameters agree reasonably with the observations.

The results emphasize the importance on the solvating and swelling properties of the solvent. Skin formation is dependent on the solution satisfying a swelling criterion (Eq. 17). The formation of well-defined pores in the backing gel is also governed by swelling.

NOTATION

A = surface area of a growing nucleus
$a, \dot{a}$ = membrane thickness and its rate of change
b = radius of a nucleus
c = concentration of a solvent
c_o = initial concentration of the solvent
D = diffusion coefficient of the solvent
D_p = diffusion coefficient of the polymer in the solution
J_p = flux of the polymer
ℓ = magnitude of the skin thickness
n = number of nuclei per unit volume
r = radial distance from the center of a nucleus
t = time
v = volume of a growing nucleus
x = coordinate in the normal direction
X = degree of gel formation, Eq. [26]
y = coordinate in the tangential direction

Greek Letters

β = rate of growth of a disturbance
κ = see Eq. 15
Λ = wavelength of the disturbance
λ = center-to-center distance between neighboring nuclei
ρ = total molar concentration
ρ_p = molar concentration of the polymer
$\rho_c = \dfrac{\partial\rho}{\partial c}$
ρ_{pg} = concentration of the polymer in the gel
ρ_{pe} = solubility of the polymer in water
ρ_{po} = initial concentration of the polymer
$\langle\rho_p\rangle$ = average polymer concentration in the solution
τ_g = times available for pore growth
τ = times for establishing pores
ω = wavenumber $2\pi\Lambda^{-1}$

Superscripts

$'$ = fluctuations
$\hat{}$ = x-dependent or constant part of the fluctuations
$*$ = quantities far from a nucleus

APPENDIX

The stability conditions under evaporation are derived for two-component solvents. The procedure follows the same method as for a single-component solvent derived in the text. The conservation equations, initial and boundary conditions for a two-component solvent are,

$$\frac{\partial c_1}{\partial t} = D_1 \frac{\partial^2 c_1}{\partial x^2} \tag{A1}$$

$$\frac{\partial c_2}{\partial t} = D_2 \frac{\partial^2 c_2}{\partial x^2} \tag{A2}$$

$$c_1\big| = c_{10} \quad t = 0 \tag{A3}$$

$$c_2\big| = c_{20} \quad t = 0 \tag{A4}$$

$$c_1 = c_2 = 0 \quad \text{on } x = 0 \tag{A5, A6}$$

$$c_1\big| = c_{10} \quad x \to \infty \tag{A7}$$

$$c_2\big| = c_{20} \quad x \to \infty \tag{A8}$$

The solutions are

$$c_1 = c_{10}\,\mathrm{erf}\left[\frac{x}{\sqrt{4D_1 t}}\right] \tag{A9}$$

$$c_2 = c_{20}\,\mathrm{erf}\left[\frac{x}{\sqrt{4D_2 t}}\right] \tag{A10}$$

Under perturbation, the conservation equations become

$$\frac{\partial c_1'}{\partial t} = D_1\left[\frac{\partial^2 c_1}{\partial x^2} + \frac{\partial^2 c_1'}{\partial y^2}\right] \tag{A11}$$

$$\frac{\partial c_2'}{\partial t} = D_2\left[\frac{\partial^2 c_2'}{\partial x^2} + \frac{\partial^2 c_2'}{\partial y^2}\right] \tag{A12}$$

subject to the conditions of zero concentration on the surface,

$$c_1'\big|_{x=0} + \frac{\partial c_1}{\partial x}\Big|_{x=0} a' = 0 \tag{A13}$$

$$c_2'\big|_{x=0} + \frac{\partial c_2}{\partial x}\Big|_{x=0} a' = 0 \tag{A14}$$

and zero concentrations far away from the surface,

$$c_1'| = 0 \qquad (A15)$$
$$x \to \infty$$
$$c_2'| = 0 \qquad (A16)$$
$$x \to \infty$$

The solutions are in the form $c_1' = \hat{c}_1(x)e^{i\omega y}e^{\beta t}$, $c_2' = \hat{c}_2(x)e^{i\omega y}e^{\beta t}$, and $a' = \hat{a}e^{i\omega y}e^{\beta t}$, and

$$\hat{c}_1 = \frac{-c_{10}\hat{a}}{\sqrt{\pi D_1 t}} \exp\left(-x\sqrt{\omega^2 + \frac{\beta}{D_1}}\right) \qquad (A17)$$

$$\hat{c}_2 = \frac{-c_{20}\hat{a}}{\sqrt{\pi D_2 t}} \exp\left(-x\sqrt{\omega^2 + \frac{\beta}{D_2}}\right) \qquad (A18)$$

The basic rate of shrinkage is obtained from the conservation of the polymer, or

$$\frac{d}{dt}\int_o^a (\rho - c_1 - c_2)dx = 0 \qquad (A19)$$

Under perturbation, one obtains a similar equation

$$\int_o^a \left[(\rho_{c_1} - 1)\frac{\partial c_1'}{\partial t} + (\rho_{c_2} - 1)\frac{\partial c_2'}{\partial t}\right] dx - (\rho - c_1 - c_2)\Big|_{x=0} a' = 0 \qquad (A20)$$

The rest is straightforward. Equations A11, A12, A17 and A18 are used to obtain

$$1 = \frac{\kappa_1}{\sqrt{\pi D_1 t}\sqrt{\frac{\beta}{D_1} + \omega^2}} + \frac{\kappa_2}{\sqrt{\pi D_2 t}\sqrt{\frac{\beta}{D_2} + \omega^2}} \qquad (A21)$$

where

$$\kappa_1 = -\left.\frac{\partial \ln(\rho - c_1 - c_2)}{\partial \ln c_1}\right|_{\substack{c_1 = c_{10} \\ c_2 = c_{20}}} \cdot \frac{\rho_p(c_1 = c_{10}, c_2 = c_{20})}{\rho_p(c_1 = 0, c_2 = 0)} \qquad (A22)$$

$$\kappa_2 = -\left.\frac{\partial \ln(\rho - c_1 - c_2)}{\partial \ln c_2}\right|_{\substack{c_1 = c_{10} \\ c_2 = c_{20}}} \cdot \frac{\rho_p(c_1 = c_{10}, c_2 = c_{20})}{\rho_p(c_1 = 0, c_2 = 0)} \qquad (A23)$$

In deriving Eq. A21, the approximations $\hat{c}_1(x = a) = \hat{c}_2(x = a) = 0$, $d\hat{c}_1/dx(x = a) = d\hat{c}_1/dx(x = a) = 0$ have been used in keeping with the assumption of small boundary layer. Further, the results that $\partial^2 c_1/\partial x^2|_{x=0} = \partial^2 c_2/\partial x^2|_{x=0} = 0$ have been used.

If 1 refers to acetone and 2 to a second component, then writing κ_2 as $\kappa_2 = -c_{20}/\rho_p(c_1 = 0, c_2 = 0)\cdot\partial(\rho - c_1 - c_2)/\partial c_2|_{c_1=c_{10},c_2=c_{20}}$ one observes that $\kappa_2 \to 0$ as $c_{20} \to 0$; in that limit Eq. A21 reduces to Eq. 13a. At small wavelengths (or large ω), Eq. A21 reduces to

$$\beta \sim 2\omega^2\left[\frac{\kappa_1}{\omega\sqrt{\pi D_1 t}} + \frac{\kappa_2}{\omega\sqrt{\pi D_2 t}} - 1\right]\cdot\left[\frac{1}{D_1} + \frac{1}{D_2}\right] - 1 \qquad (A24)$$

Although Eq. A24 looks somewhat different from Eq. 14, no features qualitatively different from a single component solvent can be obtained. Essentially choosing two component solvent provides sufficient flexibility in overcoming thermodynamic constraint such as Eq. 17, as well as providing the right evaporation rates. The constants κ_1 and κ_2 can be further modified by adding a nonvolatile inorganic salt.

Following a procedure set earlier, τ the times of pore formation is given by

$$\tau = 2\bar{\kappa}^2 - \frac{8\omega^2}{\bar{D}} - 2\bar{\kappa}\sqrt{\bar{\kappa}^2 - \frac{8\omega^2}{\bar{D}}} \qquad (A25)$$

Where $\bar{\kappa} = \kappa_1/\omega\sqrt{\pi D_1} + \kappa_2/\omega\sqrt{\pi D_2}$ and $\bar{D} = [D_1^{-1} + D_2^{-1}]^{-1}$. It is required that $\bar{\kappa}^2 > 1/2\bar{D}\omega^2$ or that

$$\left[\frac{\kappa_1}{\sqrt{\pi D_1}} + \frac{\kappa_2}{\sqrt{\pi D_2}}\right]^2 > \frac{1}{2}\left[\frac{1}{D_1} + \frac{1}{D_2}\right] \qquad (A26)$$

If ℓ is the thickness of the skin such that $\ell\sqrt{\beta/D_1 + \omega^2} \approx \ell\sqrt{\beta/D_2 + \omega^2} \approx 1$ then from Eqs. A17 and A18 and using Eq. A21

$$\ell = \frac{\kappa_1}{\sqrt{\pi D_1 \tau}} + \frac{\kappa_2}{\sqrt{\pi D_2 \tau}} \qquad (A27)$$

where time t has to be set to τ given by Eq. A25.

LITERATURE CITED

Anderson, J. E., and R. Ullman, "Mathematical Analysis of Factors Influencing the Skin Thickness of Asymmetric Reverse Osmosis Membranes," *J. Appl. Phys.*, **44**, 4303 (1973).

Cabasso, I., "Ultrastructure of Asymmetric and Composite Membranes," in *Synthetic Membranes v. I*, A. F. Turbak, ed., *ACS Symp. Ser.*, **153**, Washington, DC, 267 (1981).

Cohen, C., G. B. Tanny, and S. Prager, "Diffusion-Controlled Formation of Porous Structure in Ternary Polymer Systems," *J. Polymer Sci. Polymer Phys. Ed.*, **17**, 477 (1979).

Cooper, A. R., ed., *Ultrafiltration Membranes and Applications, Polymer Science and Technology. v. 13*, Plenum, New York (1980).

Fine, M. E., *Introduction to Phase Transformations in Condensed Systems*, Macmillan Co., New York, 53 (1964).

Katoh, M., and S. Suzuki, "Electron Microscopy of Cellulose Acetate Reverse Osmosis Membranes by Means of the Improved Replication Method," *Synthetic Membranes v. I*, A. F. Turbak, ed., *ACS Symp. Ser.*, **153**, Washington, DC, 247 (1981).

Kesting, R. E., "Membranes," *Cellulose and Cellulose Derivatives V*, N. M. Bikales and L. Segal, eds., Wiley-Interscience, New York, 1233 (1971).

Loeb, S., "Preparation and Performance of High-Flux Cellulose Acetate Desalination Membranes," *Desalination by Reverse Osmosis*, U. Merten, ed., M.I.T. Press, Cambridge, 55 (1966).

Loeb, S., and S. Sourirajan, "Sea Water Demineralization by Means of an Osmotic Membrane," *Adv. in Chemistry Ser. v. 38*, R. F. Gould, ed., American Chemical Society, Allied Pub., Washington, DC, 117 (1963).

Lonsdale, H. K., "Properties of Cellulose Acetate Membranes," *Desalination by Reverse Osmosis*, U. Merten, ed., M.I.T. Press, Cambridge, 93 (1966).

Lonsdale, H. K., and H. E. Podall, eds., *Reverse Osmosis Membrane Research*, Plenum, New York (1972).

Merten, U., ed., *Desalination by Reverse Osmosis*, M.I.T. Press, Cambridge (1966).

Miller, C. A., "Stability of Interfaces," *Surface and Colloid Science v. 10*, E. Matijevic, ed., Plenum Pub. Corp., 227 (1978).

Moore, W. R., "Concentrated Solutions," *Cellulose and Cellulose Derivatives, IV*, N. M. Bikales and L. Segal, eds., Wiley-Interscience, New York, 519 (1971).

Petty, C. A., and W. E. Stevens, "Exchange of Stability for Surface Tension Driven Flows," AIChE Ann. Mtg., Chicago (1980).

Riley, R., J. O. Gardner, and U. Merten, "Cellulose Acetate Membranes: Electron Microscopy of Structure," *Science*, **143**, 801 (1964).

Riley, R. L., U. Merten, and J. O. Gardner, "Cellulose Acetate Osmotic Membranes," *Desalination*, **1**, 30 (1966).

Sirkar, K. K., "Separation of Gaseous Mixtures with Asymmetric Dense Polymeric Membranes," *Chem. Eng. Sci.*, **32**, 1137 (1977).

Sirkar, K. K., N. K. Agarwal, and G. Pandurangaiah, "The Effect of Short Air Exposure Periods on the Performance of Cellulose Acetate Membranes From Casting Solutions with High Cellulose Acetate Content," *J. Applied Polymer Sci.*, **22**, 1919 (1978).

Sourirajan, S., *Reverse Osmosis*, Logos Press, Acad. Press, New York, 1 (1970).

Souriraran, S., ed., *Reverse Osmosis and Synthetic Membranes*, National Research Council of Canada, Ottawa (1977).

Stevens, W. E., "Theoretical Analysis of Cavitation in Polymeric Membranes during Gelation," M. S. Thesis, University of Delaware (1976).

Stevens, W. E., C. S. Dunn, and C. A. Petty, "Surface Tension Induced Cavitation in Polymeric Membranes During Gelation," AIChE Ann. Mtg., Chicago (1980).

Turbak, A. F., ed., *Synthetic Membranes v. I-II, ACS Symp. Ser.*, **153-154**, Washington, DC (1981).

Wert, C., and C. Zener, "Interferences of Growing Spherical Precipitate Particles," *J. Appl. Phys.*, **21**, 5 (1950).

Ueberreiter, K., "The Solution Process," *Diffusion in Polymers*, J. Crank and G. S. Park, eds., Acad. Press, New York, 220 (1968).

Van Hook, A., *Crystallization Theory and Practice*, Reinhold, New York, 178 (1961).

Vrentas, J. S., and J. L. Duda, "Molecular Diffusion in Polymer Solutions," *AIChE J.*, **25**, 1 (1979).

Manuscript received September 14, 1981; revision received March 4, and accepted June 18, 1982.